

A crossed molecular beams study of the reaction of the ethynyl radical ($C_2H(X^2\Sigma^+)$) with allene ($H_2CCCH_2(X^1A_1)$)

Fangtong Zhang, Seol Kim and Ralf I. Kaiser*

Received 12th December 2008, Accepted 30th January 2009

First published as an Advance Article on the web 2nd March 2009

DOI: 10.1039/b822366a

The crossed beams reaction of ground state ethynyl radicals, $C_2H(X^2\Sigma^+)$, with allene, $H_2CCCH_2(X^1A_1)$, was conducted under single collision conditions at a collision energy of 22.0 ± 0.4 kJ mol⁻¹. The center-of-mass functions were combined with earlier *ab initio* calculations and revealed that the reaction was barrier-less, proceeded *via* indirect reaction dynamics through an addition of the ethynyl radical to the terminal carbon atom of the allene molecule, and was terminated by atomic hydrogen emission *via* a tight exit transition state to form the ethynylallene product. The overall reaction was found to be exoergic by 93 ± 15 kJ mol⁻¹. Since the reaction is barrier-less, exoergic, and all transition states involved are located below the energy level of the separated reactants, the formation of ethynylallene is predicted to take place in low temperature atmospheres of planets and their satellites such as Titan and also in cold molecular clouds *via* the neutral–neutral reaction of ethynyl radicals with allene. Implications to interstellar chemistry and a comparison with the chemistry of the isoelectronic cyano radical, $CN(X^2\Sigma^+)$, are also presented.

1. Introduction

The ethynyl radical, C_2H , in its $X^2\Sigma^+$ electronic ground state has been observed in combustion systems^{1,2} and also in cold molecular clouds like the Taurus Molecular Cloud TMC-1.^{3–5} As a photodissociation product of acetylene in hydrocarbon-rich atmospheres of planets and their satellites such as Saturn's moon Titan, the ethynyl radical has also been implicated as a building block to form complex polyene-like structures.^{6,7} As a highly reactive transient species, kinetics studies indicate that this radical reacts with a broad group of molecules ranging from simple di- and triatomic molecules like molecular hydrogen (H_2),^{8,9} molecular oxygen (O_2),¹⁰ and water (H_2O)¹¹ *via* hydrocarbons^{2,12–16} to nitrogen-containing molecules as complex as nitriles^{8,15,17–19} over a broad temperature range as low as 10 K under interstellar conditions up to a few 1000 K as present in combustion flames. In combustion systems, ethynyl plays a crucial role in the synthesis of polyynes, polycyclic aromatic hydrocarbons (PAHs), and soot particles;^{1,20} the ethynyl radical has also an important impact on the NO_x chemistry in flames.^{8,21} In the vast interstellar medium, *Atacama Pathfinder Experiment* (APEX) single-dish observations reveal that ethynyl is almost omnipresent covering all stages of interstellar cloud evolution from dark clouds (molecular clouds) *via* high-mass star forming regions to protostellar objects and even ultracompact HII regions.⁵ In hydrocarbon-rich planetary and satellite atmospheres like Saturn's moon Titan, photochemical models indicate that ethynyl is the main photodissociation product of acetylene. Here, ethynyl is thought to play a central role in the chemical evolution of Titan's atmosphere and of the optically

visible brownish-orange haze layers in particular which are likely formed from simple radicals and molecules *via* polycyclic aromatic hydrocarbons (PAHs) and aerosol particles.^{22,23} Since the macroscopic alteration of combustion systems and planetary atmospheres consists of multiple elementary reactions that are in principle a series of bimolecular encounters between atoms, molecules and radicals, a detailed understanding of the mechanisms of ethynyl radical reactions at the most fundamental, microscopic level is crucial.

The importance of the ethynyl radical in Titan's atmosphere has inspired intense studies of its low temperature kinetics. Among them, the Leone group developed a cryogenically cooled flow cell as well as a pulsed Laval nozzle system coupled to a chemiluminescence or laser induced fluorescence (LIF) detection system. A systematic study of ethynyl radical reactions with various hydrocarbon species like methane (CH_4), acetylene (C_2H_2), ethylene (C_2H_4), ethane (C_2H_6), allene and methylacetylene (C_3H_4), as well as benzene (C_6H_6), was conducted covering Titan's atmospheric temperature range from 90 K to 200 K.^{12,14–16,24} The results indicated that the ethynyl radical reactions with hydrocarbons were rapid close to gas kinetics limits over the whole temperature range and proceeded without barrier; overall rate coefficients of a few 10^{-10} cm³ s⁻¹ demonstrate that these reactions are expected to have a significant impact on Titan's chemistry even at low temperatures. Parallel to these studies, Sims *et al.* utilized a *continuous* flow kinetics CRESU (Cinetique de Reaction en Ecoulement Supersonique Uniforme or reaction kinetics in uniform supersonic flow) to also investigate the kinetics of ethynyl radical reactions with hydrocarbons. Both Leone *et al.*'s and Sims *et al.*'s results correlate nicely suggesting that ethynyl radical reactions are even rapid at ultra low temperatures down to 13 K.^{12,13}

Department of Chemistry, University of Hawai'i at Manoa, Honolulu, HI 96822, USA. E-mail: ralfk@hawaii.edu

In recent years, the reactions of the ethynyl radical with methylacetylene (CH_3CCH) and its allene isomer (H_2CCCH_2) have received considerable attention. In 2001, Sims *et al.* and Leone *et al.* conducted kinetics studies of these reactions. With the pulsed Laval nozzle, the Leone group measured rapid rate constants at 103 K of $(2.7 \pm 0.6) \times 10^{-10}$ and $(2.5 \pm 0.6) \times 10^{-10} \text{ cm}^3 \text{ s}^{-1}$ for methylacetylene and allene, respectively.¹² Similarly, Sims *et al.* derived temperature dependent rate constants following $k(T) = (2.1 \pm 1.6) \times 10^{-10} (T/298 \text{ K})^{-(0.3 \pm 0.7)} \text{ cm}^3 \text{ s}^{-1}$ and $k(T) = (2.0 \pm 0.6) \times 10^{-10} (T/298 \text{ K})^{-(0.4 \pm 0.3)} \text{ cm}^3 \text{ s}^{-1}$ for methylacetylene and allene over a temperature range from 63 K to 296 K.¹³ However, these kinetics measurements do not provide the nature of the reaction products. To elucidate the nascent products of ethynyl radical reactions, crossed molecular beams experiments under single collision conditions are imperative. Here, Kaiser *et al.* conducted a study on the reaction of the D_1 -ethynyl radical with methylacetylene (CH_3CCH) and its partially deuterated isotopologues (CD_3CCH , CH_3CCD) at collision energies close to 39.8 kJ mol^{-1} .²⁵ These studies revealed that the reaction of ethynyl with methylacetylene was indirect and advanced *via* addition to the acetylenic α -carbon atom to form long-lived *cis-trans* $\text{CH}_3\text{CCH}(\text{C}_2\text{D})$ intermediates. Based on the reaction with partially deuterated molecules, two competing atomic hydrogen elimination pathways forming methyl diacetylene (CH_3CCCCH ; 70–90%) and ethynylallene ($\text{H}_2\text{CCCH}(\text{CCH})$; 10–30%) under true single collision conditions were monitored. In a more recent paper, Goulay *et al.* reported kinetics studies with product detection of the ethynyl–allene and ethynyl–methylacetylene systems. These investigations were conducted at 293 K within a slow flow reactor at about 4 Torr coupled to a multiplexed photoionization mass spectrometer; utilizing tunable vacuum ultraviolet radiation from a synchrotron, product isomers were inferred *via* their ionization potentials and fitting the corresponding photoionization efficiency curves.²⁴ The reaction of methylacetylene with ethynyl was suggested to form 50–70% diacetylene (HCCCCH) and 50–30% C_5H_4 isomers, with an isomer distribution of 15–20% ethynylallene ($\text{H}_2\text{CCCH}(\text{CCH})$) and 85–80% methyl diacetylene (CH_3CCCCH). On the other hand, the authors derived that the reaction of allene with ethynyl produced 35–45% ethynylallene ($\text{H}_2\text{CCCH}(\text{CCH})$), 20–25% methyl diacetylene (CH_3CCCCH), and 45–30% 1,4-pentadiyne (HCCCH_2CCH). It should be noted, however, that under those experimental conditions, the reaction intermediates may undergo up to a few thousand collisions with the bath molecules so that three-body encounters cannot be eliminated. Therefore, the reaction products formed under single collision conditions still remain to be ascertained in case of the ethynyl–allene system. Here, we expanded our previous crossed beams investigations from the ethynyl–methylacetylene to the ethynyl–allene reaction. The present studies utilize a newly developed photolytic ethynyl source. To test this new supersonic source, we first reexamined the ethynyl–methylacetylene reaction as a reference system and conducted thereafter the crossed beams reaction of the ethynyl radical with allene and its D_4 -isotopologue. These data are interpreted in light of earlier electronic structure calculations of these systems.⁷

2. Experimental and data analysis

The reactions of the ground state ethynyl radical, $\text{C}_2\text{H}(\text{X}^2\Sigma^+)$, with methylacetylene, $\text{CH}_3\text{CCH}(\text{X}^1\text{A}_1)$, and allene, $\text{H}_2\text{CCCH}_2(\text{X}^1\text{A}_1)$, were conducted in a universal crossed molecular beams machine under single collision conditions at the University of Hawai'i. The experimental setup has been described in detail elsewhere.^{26–29} A supersonic beam of ethynyl radicals, $\text{C}_2\text{H}(\text{X}^2\Sigma^+)$, was generated in the primary source *via* photodissociation of helium-seeded bromoacetylene (C_2HBr). The bromoacetylene precursor was entrained in helium (99.9999%, Airgas) at a ratio of 1%. The gas mixture was released by a Proch–Trickl pulsed valve operating with a 0.1 mm nozzle at 60 Hz, 80 μs pulse width, -500 V pulse amplitude, and 700 Torr backing pressure. During these operation conditions, the pressure in the primary source increased to about 2×10^{-5} Torr. The distance between the nozzle and the skimmer was optimized to be 12 mm. A Teflon extension with a slit located parallel to the expansion direction of the pulsed beam was interfaced to the end of the nozzle; this allowed a 193 nm laser beam focused to 2 mm by 5 mm from a Lambda Physik Compex 110 Excimer laser operated at 30 Hz and 35–40 mJ per pulse to intercept the bromoacetylene beam perpendicularly and 5 mm downstream of the nozzle. This was assisted by passing the excimer laser output (25 mm \times 10 mm) first through a 2:1 beam condenser and then through a 1000 mm fused silica lens. Note that higher concentrations of bromoacetylene must be avoided to eliminate the formation of diacetylene as the product of ethynyl radical self-recombination. About 6% of the bromoacetylene precursor molecules were photodissociated in this process to generate an ethynyl radical and a bromine atom; both species were seeded in the helium gas. Since the lifetime of the $\text{A}^2\text{A}'$ state is less than 1 μs , any $\text{C}_2\text{H}(\text{A}^2\text{A}')$ species will relax while traveling from the photolysis center to the interaction region.

After passing a skimmer, a four-slot chopper wheel selected a part of the ethynyl beam at a peak velocity, v_p , of $1490 \pm 20 \text{ ms}^{-1}$ and a speed ratio, S , of 8.5 ± 0.5 . This segment of the ethynyl beam crossed a pulsed hydrocarbon beam from the secondary source. Distinct experiments were conducted with methylacetylene (CH_3CCH , 99.9%, Organic Technologies; 550 Torr; $v_p = 820 \pm 20 \text{ ms}^{-1}$; $S = 13.0 \pm 0.2$), allene (H_2CCCH_2 , 97%+, Sigma-Aldrich; 550 Torr; $v_p = 810 \pm 20 \text{ ms}^{-1}$; $S = 13.0 \pm 0.2$), and D_4 -allene (D_2CCCD_2 , 99%, CDN; 350 Torr; $v_p = 800 \pm 20 \text{ ms}^{-1}$; $S = 13 \pm 0.2$) released by a second pulsed valve perpendicular to the interaction region. This pulsed valve operated with a 0.1 mm nozzle at 60 Hz, 80 μs pulse width, -500 V pulse amplitude, and a nozzle–skimmer distance of 12 mm. Collision energies of $22.1 \pm 0.4 \text{ kJ mol}^{-1}$ (methylacetylene), $22.0 \pm 0.4 \text{ kJ mol}^{-1}$ (allene), and $22.8 \pm 0.4 \text{ kJ mol}^{-1}$ (D_4 -allene) were obtained. During the actual experiments, the pressure in the secondary source was about 1×10^{-4} Torr. Note that to optimize the intensity of each supersonic beam, which strongly depends on the distance between the pulsed valve and the skimmer, on line and *in situ*, each pulsed valve was placed on an ultra high vacuum compatible micro positioning translation stage with three stepper motors (New Focus). This allows monitoring

of the beam intensity *versus* the position of the pulsed valve in each source chamber in real time.

The reactively scattered species were monitored using a triply differentially pumped quadrupole mass spectrometric detector in the time-of-flight (TOF) mode after electron-impact ionization of neutral species at 80 eV electron energy. This detector can be rotated within the plane defined by the primary and the secondary reactant beams to allow the taking of angular resolved TOF spectra. At each angle, up to 1.5×10^6 TOF spectra (up to 15 hours per angle) were accumulated; due to the costs of deuterated chemicals, TOF data were taken for the ethynyl-D₄-allene system only at the corresponding center-of-mass angle. The recorded TOF spectra were then integrated and normalized to extract the product angular distribution in the laboratory frame (LAB). Note that the operation of the primary and secondary pulsed valves at 60 Hz and the photodissociation laser at only half the repetition rate of 30 Hz allows a background subtraction by taking TOF spectra in the 'laser on' mode and subtracting from the TOF spectra recorded on the 'laser off' mode. To collect information on the scattering dynamics, the laboratory data were transformed into the center-of-mass reference frame utilizing a forward-convolution routine.^{30,31} This iterative method initially assumes an angular flux distribution, $T(\theta)$, and a translational energy flux distribution, $P(E_T)$, in the center-of-mass system (CM). Laboratory TOF spectra and the laboratory angular distributions (LAB) are then calculated from the $T(\theta)$ and $P(E_T)$ functions and are averaged over a grid of Newton diagrams to account for the apparatus functions and the beam spreads. Each diagram defines, for instance, the velocity and angular spread of each beam and the detector acceptance angle. Best fits were obtained by iteratively refining the adjustable parameters in the center-of-mass functions within the experimental error limits of, for instance, peak velocity, speed ratio, error bars in the LAB distribution.

The bromoacetylene precursor was synthesized according to an adapted literature procedure.^{32,33} Briefly, amber glassware was employed in the synthesis to ensure that the bromoacetylene is not decomposed by light. First, 7 mL of 1,2-dibromoethylene were mixed with 15 mL of ethanol. The mixture was then dropwise added over 60 min to aqueous sodium hydroxide (NaOH) solution and refluxed for 90 min. The evolving gaseous products were carried away by helium carrier gas and trapped into a liquid nitrogen cooled cold trap. The crude sample frozen inside the trap was then isolated, evacuated, and purified by trap-to-trap distillation. Gas mixtures of 1% bromoacetylene in helium (99.9999%, Airgas) were prepared at room temperature at a total pressure of about 8.5 atm. These mixtures were stored in Teflon-coated stainless steel gas cylinders (Matheson Trigas) and were found to be stable for weeks. The purity of the bromoacetylene sample was characterized *via* mass spectrometry and infrared spectroscopy. Briefly, mass spectra of the samples were taken with a quadrupole mass spectrometer (Balzer) operated at 100 eV electron energy, 0.3 mA electron current, and with a secondary electron multiplier voltage of 2000 V over a mass range from 10 to 200 amu. The mass spectrum was dominated by the parent

Table 1 Peak assignment of the mass spectrum of bromoacetylene (C₂HBr) and ions originating from the dibromoethylene molecule as shown in Fig. 1

m/z	Assignment	Relative intensity (%)
12	C ⁺	8
13	CH ⁺	2
24	C ₂ ⁺	8
25	C ₂ H ⁺	59.5
52	C ₂ H ⁷⁹ Br ²⁺	7
53	C ₂ H ⁸¹ Br ²⁺	5.5
79	⁷⁹ Br ⁺	12
80	H ⁷⁹ Br ⁺	5.5
81	⁸¹ Br ⁺	10.5
82	H ⁸¹ Br ⁺	4.5
91	C ⁷⁹ Br ⁺	3
93	C ⁸¹ Br ⁺	3
103	C ₂ ⁷⁹ Br ⁺	6.5
104	C ₂ H ⁷⁹ Br ⁺	100
105	¹² C ¹³ CH ⁷⁹ Br ⁺ /C ₂ ⁸¹ Br ⁺	11
106	C ₂ H ⁸¹ Br ⁺	98
107	¹² C ¹³ CH ⁸¹ Br ⁺	3
158	⁷⁹ Br ₂ ⁺	0.1
160	⁷⁹ Br ⁸¹ Br ⁺	0.1
162	⁸¹ Br ₂ ⁺	0.1
184	C ₂ H ₂ ⁷⁹ Br ₂ ⁺	1
186	C ₂ H ₂ ⁷⁹ Br ⁸¹ Br ⁺	1
188	C ₂ H ₂ ⁸¹ Br ₂ ⁺	1

peaks of the bromoacetylene at mass-to-charge (m/z) ratios of $m/z = 104$ (C₂H⁷⁹Br⁺) and $m/z = 106$ (C₂H⁸¹Br⁺); ¹³C isotope peaks were detected at $m/z = 105$ (¹²C¹³CH⁷⁹Br⁺/C₂⁸¹Br⁺) and $m/z = 107$ (¹²C¹³CH⁸¹Br⁺). The ions detected at lower mass-to-charge ratios were attributed to fragments formed during the dissociative ionization of the bromoacetylene precursor molecule (Table 1). These patterns agree very well with previous mass spectral data obtained at an electron energy of 70 eV.³⁴ Only minor impurities of the dibromoethylene reactant were monitored; accounting quantitatively for the ion counts of the parents and fragments, we derive purities of the bromoacetylene sample of 99.5% +.

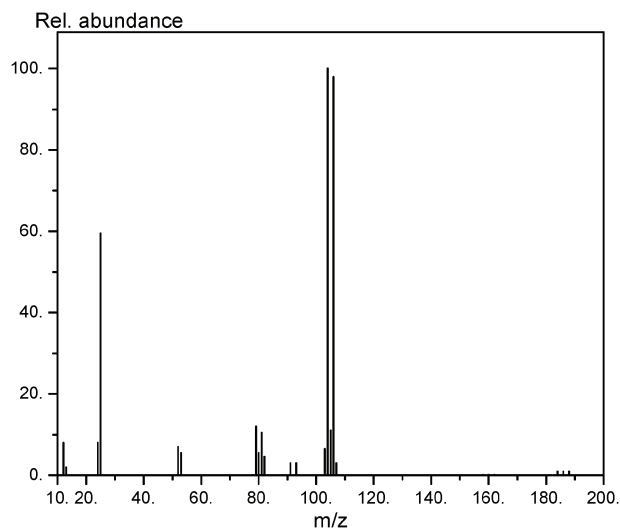


Fig. 1 Mass spectrum of bromoacetylene (C₂HBr); the spectrum is presented in a NIST standardized format. The assignment of the ions is compiled in Table 1.

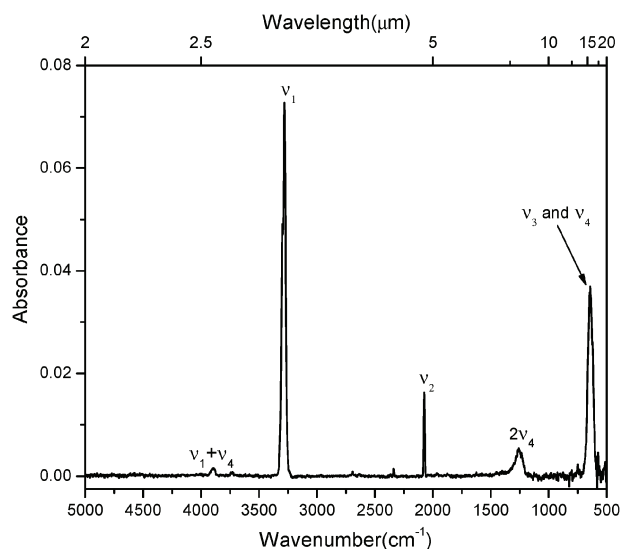


Fig. 2 Infrared spectrum of amorphous bromoacetylene ice recorded at 10 K. Positions of fundamentals, overtones, and combination bands are marked and compiled in Table 2.

Table 2 Positions of fundamentals, overtones, and combination bands of amorphous bromoacetylene ice recorded at 10 K. Units of the absorptions are given in cm^{-1} . Literature values are taken from ref. 36 (column 2) and 37 (column 3)

Amorphous (10 K)	Literature (gas phase) ³⁶	Literature (gas phase) ³⁷	Assignment	Carrier
3897	—	3935	$\nu_1 + \nu_4$	Combination
3297, 3280	3325	3336	ν_1	CH stretch
2074	2085	2091	ν_2	C≡C stretch
1256	—	1221	$2\nu_4$	Overtone
645	618	620	ν_3	CBr stretch
645	618	617	ν_4	CCH bend
—	295	291	ν_5	CCBr bend

The bromoacetylene sample was also characterized *via* infrared spectroscopy.³⁵ Briefly, the helium–bromoacetylene mixture was introduced into an ultra high vacuum machine (background pressure: few 10^{-11} Torr) and condensed for 10 min at a pressure of 10^{-7} Torr onto a silver mirror cooled by a closed cycle helium refrigerator to 10 K. The infrared spectra were taken in absorption–reflection–absorption spectroscopy of the amorphous bromoacetylene sample. Note that at these temperatures, helium does not condense on the silver mirror, but only bromoacetylene. The infrared spectrum of the bromoacetylene sample and the positions of the fundamentals, combination bands, and overtones agree very well with previous gas phase studies^{36,37} (Fig. 2; Table 2). Note that the ν_5 fundamental could not be monitored due to the cutoff of our liquid nitrogen cooled DTGS detector at about $450\text{--}500\text{ cm}^{-1}$.

3. Results

3.1 Laboratory data

In both the methylacetylene and allene experiments, we probed the reactive scattering signal at mass-to-charge ratios

of $m/z = 64$ (C_5H_4^+), 63 (C_5H_3^+), 62 (C_5H_2^+), 61 (C_5H^+) and 60 (C_5^+). No reactive scattering signal at $m/z = 50$ (C_4H_2^+) was detected. All the TOF spectra at $m/z = 64$ (C_5H_4^+) and lower mass-to-charge ratios were superimposable after scaling. This finding alone suggests that the molecular hydrogen and methyl group elimination channels are closed and that the signal at lower mass-to-charge ratios originated within our detection limit solely from a dissociative ionization of the C_5H_4 parent molecule in the ionizer of the detector. Therefore, for both systems, the only channel open at collision energies of about 22 kJ mol^{-1} in the present mass range is the formation of a product of the gross formula C_5H_4 together with the light hydrogen atom. Note that the finding in the case of the ethynyl–methylacetylene system agrees well with a previous study under single collision conditions at a collision energy of 39 kJ mol^{-1} .²⁵ Our earlier study also utilized partially deuterated methylacetylene reactants demonstrating that two channels are open: a hydrogen loss from the methyl group and from the acetylenic group leading to ethynylallene ($\text{H}_2\text{CCCH}(\text{CCH})$) and methylacetylene (CH_3CCCCH). In case of the ethynyl–allene reaction, the

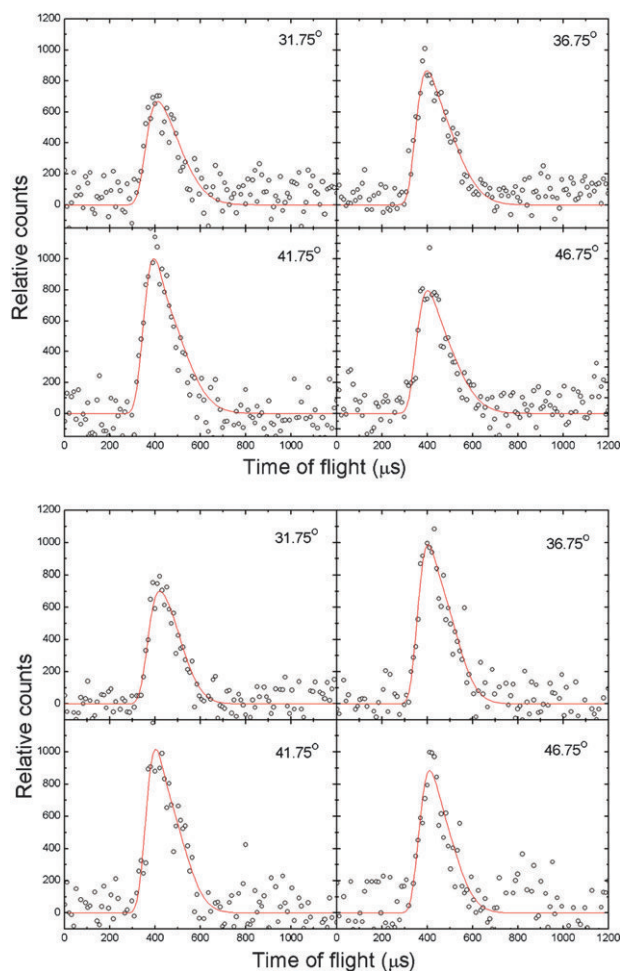


Fig. 3 Selected time-of-flight (TOF) spectra of $m/z = 64$ (C_5H_4^+) recorded at collision energies of 22.1 and 22.0 kJ mol^{-1} at various laboratory angles for the reactions of ethynyl radical with methylacetylene (upper panel) and allene (lower panel). The circles indicate the experimental data; the solid lines, the calculated fits.

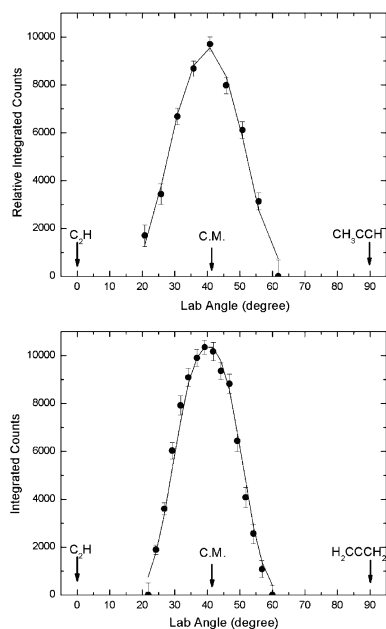


Fig. 4 Laboratory angular distributions (LAB) of the C_5H_4 product recorded at $m/z = 64$ ($C_5H_4^+$) at collision energies of 22.1 and 22.0 kJ mol^{-1} for the reactions of ethynyl radical with methylacetylene (upper panel) and allene (lower panel). Circles and error bars indicate experimental data, and the solid line the calculated distribution with the best-fit center-of-mass functions.

eliminated hydrogen atom could originate from the allene or from the ethynyl radical. Therefore, we conducted a crossed beams reaction of ethynyl with D_4 -allene. A hydrogen atom loss from the ethynyl group should result in a scattering signal at $m/z = 68$ ($C_5D_4^+$); on the other hand, a deuterium loss should be monitored *via* a signal at $m/z = 67$ ($C_5HD_3^+$). It is important to note that $m/z = 68$ ($C_5D_4^+$) cannot fragment to $m/z = 67$ ($C_5HD_3^+$), but only to $m/z = 66$ ($C_5D_3^+$) and lower. Our experiments with D_4 -allene depicted explicitly that only ion counts at $m/z = 67$ ($C_5HD_3^+$) were detectable; therefore, this experiment verifies that the ethynyl

group stays intact, and that in the case of the ethynyl–allene system, the emitted hydrogen atom must originate from the allene molecule.

For the ethynyl–allene and ethynyl–methylacetylene systems, the TOF spectra at selected laboratory angles together with the best fits are shown in Fig. 3. The corresponding laboratory (LAB) angular distributions recorded at $m/z = 64$ ($C_5H_4^+$) are depicted in Fig. 4. For both reactions, the distributions look similar and spread over about 40° in the scattering plane defined by both beams. Also, both distributions are nearly symmetric with respect to the center-of-mass angles of $41.0^\circ \pm 0.5^\circ$ and $41.2^\circ \pm 0.5^\circ$, respectively; further, they show distribution maxima close to the center-of-mass angles. This finding alone likely indicates indirect scattering dynamics *via* complex formation.

3.2 Center-of-mass distributions

Having discussed the laboratory data, we are turning our attention now to the center-of-mass angular ($T(\theta)$) and translational energy distributions ($P(E_T)$) (Fig. 5). Most importantly, for both reactions the laboratory data could be fit with only a single channel of the mass combination 64 amu (C_5H_4) and 1 amu (H). The center-of-mass translational energy distributions provide important information for the extraction of the chemical dynamics data of the ethynyl–methylacetylene and ethynyl–allene systems. First, both $P(E_T)$ s peak away from zero translational energy and depict relatively broad distribution maxima located at about 35–55 kJ mol^{-1} (methylacetylene) and 25–35 kJ mol^{-1} (allene). This finding indicates that for each system, the exit channel leading to the formation of the C_5H_4 isomer is tight involving a significant exit barrier. Secondly, for the best-fit functions, the maximum translational energies, E_{max} , are derived to be 170 kJ mol^{-1} and 115 kJ mol^{-1} for reactions with methylacetylene and allene, respectively. Our error analysis indicates that the tails of the $P(E_T)$ s can be either extended or cut by up to about 10 to 15 kJ mol^{-1} without significantly changing the results of the fit. Since the maximum

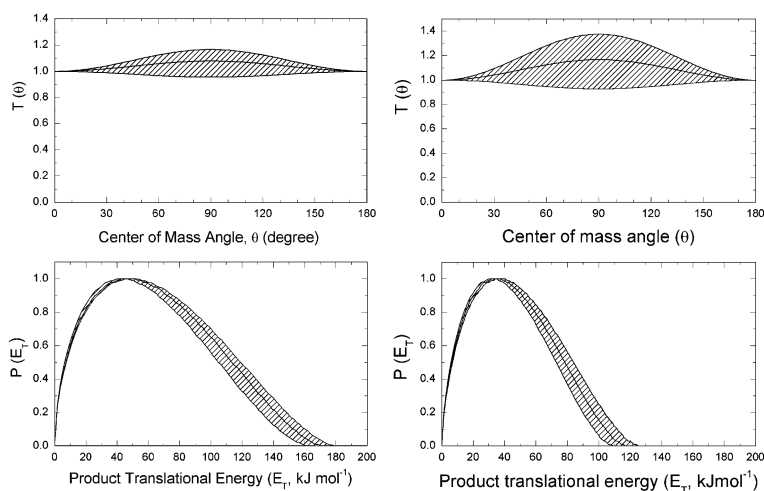


Fig. 5 Center-of-mass angular (top) and translational energy flux distributions (bottom) of the C_5H_4 plus atomic hydrogen loss channel of the reaction of ethynyl radical with methylacetylene and allene (left and right columns, respectively). Hatched areas indicate the acceptable upper and lower error limits of the fits.

translational energy presents the sum of the collision energy and the absolute of the exoergicity of the reaction, the value of E_{\max} can be used to extract the reaction exoergicity. Thus, we determine that the formation of C_5H_4 plus a hydrogen atom is exoergic by $148 \pm 15 \text{ kJ mol}^{-1}$ (methylacetylene reaction) and $93 \pm 15 \text{ kJ mol}^{-1}$ (allene reaction). From these center-of-mass translational energy distributions, we can also compute the fraction of the energy channeling into the translational modes of the products, *i.e.* $\langle E_T \rangle / E_{\max}$ with $\langle E_T \rangle$ being the averaged translational energy of the products. This suggests fractions of about $39 \pm 3\%$ for both systems. This order of magnitude is consistent with indirect scattering dynamics.³⁸

The derived center-of-mass angular distributions for both systems are very similar. In both cases, the center-of-mass angular distributions depict flux over the whole scattering range from 0° to 180° ; also, they are forward-backward symmetric with respect to 90° and only weakly polarized. Within the error limits, the laboratory data could be fit with distributions exhibiting shallow minima or even maxima at 90° ; both best-fit functions are close to isotropic distributions. These findings indicate that both the ethynyl-methylacetylene

and ethynyl-allene systems involve indirect scattering dynamics *via* the formation of bound C_5H_5 reaction intermediates.³⁹ Also, the inherent forward-backward symmetry of the $T(\theta)$ s suggests that the lifetime of the decomposing reaction intermediates is longer than their corresponding rotational period.⁴⁰ It should be noted that in principle, this forward-backward symmetry can also arise when a ‘symmetric’ intermediate rotating about an n -fold axis fragments.⁴¹ In this case, a rotational axis would interconvert two hydrogen atoms; this leads to an emission of atomic hydrogen with equal probability into θ° and $\pi - \theta^\circ$ and would result in a forward-backward symmetric center-of-mass angular distribution. However, the underlying potential energy surfaces (PES) exclude this option (Fig. 6) as no ‘symmetric’ reaction intermediate exists which correlates with the formation of energetically accessible C_5H_4 isomers. Finally, it should be noted that the mild polarization is an effect of the poor coupling between the initial and final orbital angular momentum due to the light mass of the departing hydrogen atom.³⁹ Here, angular momentum conservation dictates that most of the initial orbital angular momentum channels into the rotational excitation of the polyatomic product, here the C_5H_4 isomers.

4. Discussion

To expose the actual reaction mechanism(s), we first have to elucidate the reaction product(s). For this we compare the experimentally determined reaction energies (Section 3.2) with those of distinct isomers determined by *ab initio* calculations.^{7,25} First of all, as noted in the results section, under single collision conditions, the hydrogen atom elimination pathways are open; therefore, we will focus on energetics of the product isomers of the general formula C_5H_4 . Recall that the formation of the C_5H_4 isomer plus atomic hydrogen was found to be exoergic by about $148 \pm 15 \text{ kJ mol}^{-1}$ (methylacetylene reaction) and $93 \pm 15 \text{ kJ mol}^{-1}$ (allene reaction). Since the reaction of methylacetylene with ethynyl has already been studied previously in our group (recall that this reaction here acts as a reference system to test the ethynyl radical source), this discussion primarily focuses on the allene reaction. Findings for the methylacetylene-ethynyl system are compiled briefly and discussed in light of our earlier investigation.

For the ethynyl-methylacetylene reaction, two C_5H_4 isomers are energetically accessible: ethynylallene (**p1**) and methyladiacetylene (**p2**) formed with reaction exoergicities of $111 \pm 10 \text{ kJ mol}^{-1}$ and $133 \pm 10 \text{ kJ mol}^{-1}$, respectively. A comparison of the experimental data with the *ab initio* values suggests that **p2** is the most likely major reaction product. However, we cannot exclude additional contributions of **p1** based on these data alone. Recall that crossed beams reactions with D_3 -methylacetylene and D_1 -methylacetylene accounted explicitly for the formation of both methyladiacetylene and ethynylallene with the thermodynamically favorable methyladiacetylene molecule being the dominant product.²⁵

We can correlate the structures of the reaction products with those of the reactants, and combine the potential energy

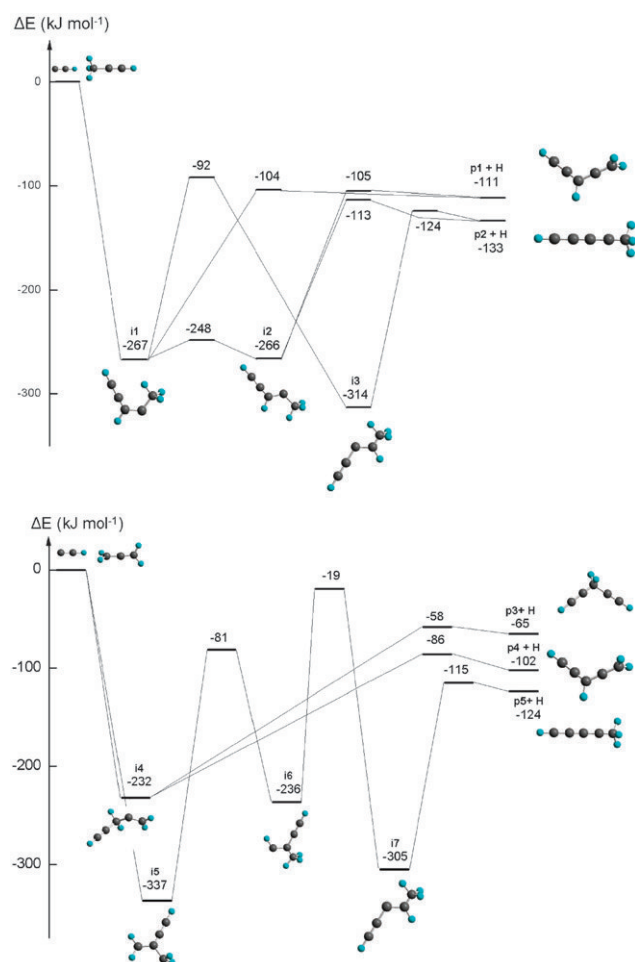


Fig. 6 a: Potential energy for the reaction of the ethynyl radical with methylacetylene as compiled from ref. 7. Uncertainties of the computed energies are 10 kJ mol^{-1} . b: Potential energy for the reaction of the ethynyl radical with allene as compiled from ref. 7. Uncertainties of the computed energies are 10 kJ mol^{-1} .

surface with the results of the crossed beams studies to propose the reaction mechanisms. The electronic structure calculations suggest that the ethynyl radical adds *via* its radical center without barrier to the sterically more accessible α -carbon atom of the methylacetylene molecule forming the initial collision complex [i1]. Recall that the center-of-mass angular distribution predicted the existence of indirect scattering dynamics and hence the involvement of reaction intermediate(s). This intermediate can either undergo *cis*–*trans* isomerization to [i2] or a hydrogen shift to yield [i3]. These structures can decompose *via* atomic hydrogen atom emission to yield methylacetylene (from [i2] and [i3]) and ethynylallene (from [i1] and [i2]). Note that the center-of-mass translational energy distribution of our present and earlier studies predicted tight exit transition states. Both exit transition states to form methylacetylene were found to be rather tight, whereas the exit transition states leading to ethynylallene are—relatively speaking—pretty loose and located only up to 7 kJ mol⁻¹ above the separated products. Also, the reactions with partially deuterated reactants²⁵ indicated that methylacetylene was the dominating isomer. The dominance of methylacetylene *versus* ethynylallene has also been verified in recent kinetics studies coupled with product detection based on the inherent ionization potentials by the Leone group.²⁴ To summarize, both previous and novel kinetics and dynamics studies are consistent and suggest that considering the C₅H₄ isomers, methylacetylene and ethynylallene are formed with methylacetylene being the dominant product. This finding correlates with the predicted relative stability of both isomers where the methylacetylene isomer is more stable by about 22 kJ mol⁻¹ compared to ethynylallene.

Considering the ethynyl–allene system, the electronic structure calculations predict three low-energy isomers of C₅H₄ (p3–p5). It is important to note that in all cases, the ethynyl unit is conserved and formally connected to the α -carbon atom of the allene unit. This correlates nicely with the finding of the D₄-allene reaction that the ethynyl unit does not fragment *via* hydrogen atom emission, and that only a deuterium atom elimination from the D₄-allene reactant was observable. However, compared to the methylacetylene system, the terminal hydrogen atoms are chemically equivalent. Therefore, it is not feasible to explicitly use partially deuterated allene reactants to pin down the product isomer(s) formed. Therefore, we turn first to a comparison of the experimentally derived reaction energy with the computed data. Here, the electronic structure calculations predict that the formation of p3 (1,4-pentadiyne), p4 (ethynylallene), and p5 (methylacetylene) is exoergic by 66 ± 10 kJ mol⁻¹, 102 ± 10 kJ mol⁻¹, and 124 ± 10 kJ mol⁻¹, respectively. Comparing with experimental data of 93 ± 15 kJ mol⁻¹, p4 (ethynylallene) is most likely the dominating pathway. However, the energetics of p5 is pretty close to the error limits of the investigations. Therefore, we investigated how sensitive our one channel fit is to the incorporation of a second pathway leading also to a C₅H₄ isomer plus a hydrogen atom. Here, we find that the fits are insensitive to an additional channel (10–20%) with a reaction exoergicity of 66 ± 15 kJ mol⁻¹ leading to the formation of the p3 (1,4-pentadiyne) structure. The contribution of the methylacetylene isomer presents a

tricky problem. We could extend the translational energy distribution with a minor intensity of about 0.02 to account for the energetics of p5 (methylacetylene). However, this contribution can also be left out without changing the fits at all. Therefore, based on the energetics, we propose that p4 (ethynylallene) is likely the dominant isomer formed with p3 (1,4-pentadiyne) having contributions of up to 20%. The involvement of p5 (methylacetylene) remains unresolved so far. These findings agree qualitatively with those of the Leone group.²⁴ Here, the authors suggested a dominating formation of 35–45% p4 (ethynylallene) with a lower fraction of 20–25% p5 (methylacetylene) and 45–30% p3 (1,4-pentadiyne).

We are combining now the experimental data and energetic considerations with the computed electronic structure calculations (Fig. 6b). Here, the C₅H₅ intermediates ([i4] and [i5]) can be formed by a barrier-less addition of ethynyl radical to either the terminal or central carbon atom of the allene molecule. Both p4 and p3 can be formed *via* hydrogen loss from the [i4] intermediate in one step through a simple addition–elimination mechanism involving exit barriers of 8 and 16 kJ mol⁻¹, respectively. A similar addition–elimination reaction was also found in the related reaction of cyano radicals CN(X²Σ⁺) with allene.^{42,43} On the other hand, the formation of p5 requires two additional isomerizations: a hydrogen shift connecting [i5] to [i6] and a methyl group migration leading from [i6] to [i7]. Based on these pathways, reactions through intermediate [i4] are clearly preferred since they involve only a single step to product formation (addition–elimination reaction) and since the addition of the ethynyl radical is directed toward the sterically more accessible terminal carbon atom of the allene molecule holding a larger cone of acceptance compared to the central carbon atom of allene. Therefore, p5 (methylacetylene) presents most likely only a minor reaction product. Recall that in the related cyano–methylacetylene and cyano–allene reactions, a methyl group migration was not observed under single collision conditions. It is important to mention that we have no evidence for the formation of p5 (methylacetylene) in contrast to previous kinetics studies.²⁴ Also, the kinetics study suggests that p4 (ethynylallene) and p3 (1,4-pentadiyne) are formed in similar quantities. We could not fit our data with the branching ratio derived from this kinetics study. It should be stressed that these slow flow studies were not conducted under single collision conditions; the collision intermediates may undergo up to a few thousand collisions. This in turn influences the internal energy of the reaction intermediates. By diverting the internal energy in consecutive reactions with both molecules, the lifetime of the reaction intermediate might be enhanced. This might switch the product spectrum.

5. Conclusion

We have studied the crossed molecular beams reaction of ground state ethynyl radicals, C₂H(X²Σ⁺), with allene, H₂CCCH₂(X¹A₁), under single collisions. For the ethynyl–allene system, the formation of ethynylallene plus atomic hydrogen was elucidated. The underlying chemical dynamics were found to be indirect, involved C₅H₅ intermediates, and were dominated by an initial barrier-less addition

of the ethynyl radical to the terminal carbon atom of the allene molecule. This initial collision complex would then decompose to yield the ethynylallene product plus atomic hydrogen through a tight exit transition state. The ethynylallene isomer was found to be the major isomer formed with 1,4-pentadiyne possibly contributing up to 20%. A third feasible reaction pathway involving the initial addition of the ethynyl radical to the central carbon atom of allene followed by a hydrogen shift and a methyl group migration to form methyldiacetylene plus atomic hydrogen was found to be an insignificant contributor at most—at least under single collision conditions. These reaction mechanisms are very similar to those of isoelectronic cyano radicals with the allene system.^{42,44} Both reactions are exoergic, have no entrance barrier, and proceed *via* indirect reaction dynamics which involve an addition of the radicals to the terminal carbon atom of the unsaturated carbon-carbon bond to form intermediates followed by an atomic hydrogen emission through exit barriers lying below the energy level of separate reactants to form at least two different isomers. Due to these reaction dynamics, these reactions are likely to happen even in low temperature environments as in Titan's atmosphere and in molecular clouds. Therefore it provides a possible route to form ethynylallene in these low temperature environments.

Acknowledgements

This work was supported by the US National Science Foundation 'Collaborative Research in Chemistry Program' (NSF-CRC; CHE-0627854). We would also like to thank Coherent, Inc. for support.

References

- R. P. Lindstedt and G. Skevis, *Combust. Sci. Technol.*, 1997, **125**, 73.
- B. Ceursters, H. M. T. Nguyen, M. T. Nguyen, J. Peeters and L. Vereecken, *Phys. Chem. Chem. Phys.*, 2001, **3**, 3070.
- C. Helling, U. G. Joergensen, B. Plez and H. R. Johnson, *Astron. Astrophys.*, 1996, **315**, 194.
- E. Herbst and C. M. Leung, *Astrophys. J., Suppl. Ser.*, 1989, **69**, 271.
- H. Beuther, D. Semenov, T. Henning and H. Linz, *Astrophys. J.*, 2008, **675**, L33.
- M. C. Gazeau, Y. Benilan, P. Coll, A. Jolly, V. Vuitton and F. Raulin, *Eur. Space Agency, [Spec. Publ.] ESA SP*, 2002, **SP-518**, 349.
- F. Stahl, P. v. R. Schleyer, H. F. Schaefer III and R. I. Kaiser, *Planet. Space Sci.*, 2002, **50**, 685.
- J. Peeters, H. Van Look and B. Ceursters, *J. Phys. Chem.*, 1996, **100**, 15124.
- J. Peeters, B. Ceursters, H. M. T. Nguyen and M. T. Nguyen, *J. Chem. Phys.*, 2002, **116**, 3700.
- S. Lee and S. R. Leone, *Chem. Phys. Lett.*, 2000, **329**, 443.
- S. A. Carl, H. M. T. Nguyen, R. M. I. Elsamra, M. T. Nguyen and J. Peeters, *J. Chem. Phys.*, 2005, **122**, 114307.
- A. B. Vakhtin, D. E. Heard, I. W. M. Smith and S. R. Leone, *Chem. Phys. Lett.*, 2001, **344**, 317.
- D. Carty, V. Le Page, I. R. Sims and I. W. M. Smith, *Chem. Phys. Lett.*, 2001, **344**, 310.
- F. Goulay and S. R. Leone, *J. Phys. Chem. A*, 2006, **110**, 1875.
- B. Nizamov and S. R. Leone, *J. Phys. Chem. A*, 2004, **108**, 1746.
- A. B. Vakhtin, D. E. Heard, I. W. M. Smith and S. R. Leone, *Chem. Phys. Lett.*, 2001, **348**, 21.
- S. A. Carl, R. M. I. Elsamra, R. M. Kulkarni, H. M. T. Nguyen and J. Peeters, *J. Phys. Chem. A*, 2004, **108**, 3695.
- B. Nizamov and S. R. Leone, *J. Phys. Chem. A*, 2004, **108**, 3766.
- Z.-X. Zhao, J.-Y. Liu, L. Wang, H.-X. Zhang, C.-Y. Hou and C.-C. Sun, *J. Phys. Chem. A*, 2008, **112**, 8455.
- J. H. Kiefer, W. A. Von Drasek and W. A. Von Drasek, *Int. J. Chem. Kinet.*, 1990, **22**, 747.
- S. A. Carl, H. M. T. Nguyen, M. T. Nguyen and J. Peeters, *J. Chem. Phys.*, 2003, **118**, 10996.
- Y. L. Yung, M. Allen and J. P. Pinto, *Astrophys. J., Suppl. Ser.*, 1984, **55**, 465.
- D. Toublanc, J. P. Parisot, J. Brillet, D. Gautier, F. Raulin and C. P. McKay, *Icarus*, 1995, **113**, 2.
- F. Goulay, D. L. Osborn, C. A. Taatjes, P. Zou, G. Meloni and S. R. Leone, *Phys. Chem. Chem. Phys.*, 2007, **9**, 4291.
- R. I. Kaiser, C. C. Chiong, O. Asvany, Y. T. Lee, F. Stahl, P. v. R. Schleyer and H. F. Schaefer III, *J. Chem. Phys.*, 2001, **114**, 3488.
- Y. Guo, X. Gu and R. I. Kaiser, *Int. J. Mass Spectrom.*, 2006, **249/250**, 420.
- Y. Guo, X. Gu, E. Kawamura and R. I. Kaiser, *Rev. Sci. Instrum.*, 2006, **77**, 034701.
- X. B. Gu, Y. Guo, E. Kawamura and R. I. Kaiser, *Rev. Sci. Instrum.*, 2005, **76**, 083115.
- X. Gu, Y. Guo and R. I. Kaiser, *Int. J. Mass Spectrom.*, 2005, **246**, 29.
- M. Vernon, PhD thesis, University of California, Berkeley, 1981.
- M. S. Weiss, PhD thesis, University of California, Berkeley, 1986.
- L. A. Bashford, H. J. Emeleus and H. V. A. Briscoe, *J. Chem. Soc.*, 1938, 1358.
- A. H. Laufer, *J. Phys. Chem.*, 1979, **83**, 2683.
- E. Kloster-Jensen, C. Pascual and J. Vogt, *Helv. Chim. Acta*, 1970, **53**, 2109.
- C. J. Bennett and R. I. Kaiser, *Astrophys. J.*, 2007, **660**, 1289.
- O. Vaittinen, T. Lukka, L. Halonen, H. Burger and O. Polanz, *J. Mol. Spectrosc.*, 1995, **172**, 503.
- G. R. Hunt and M. K. Wilson, *J. Chem. Phys.*, 1961, **4**, 1301.
- R. I. Kaiser, *Chem. Rev.*, 2002, **102**, 1309.
- R. D. Levine, *Molecular Reaction Dynamics*, Cambridge University Press, Cambridge, UK, 2005.
- W. B. Miller, S. A. Safron and D. R. Herschbach, *Discuss. Faraday Soc.*, 1967, **44**, 108.
- R. I. Kaiser, C. Oschensfeld, M. Head-Gordon, Y. T. Lee and A. G. Suits, *Science*, 1996, **274**, 1508.
- N. Balucani, O. Asvany, R. I. Kaiser and Y. Osamura, *J. Phys. Chem. A*, 2002, **106**, 4301.
- N. Balucani, O. Asvany, L. C. L. Huang, Y. T. Lee, R. I. Kaiser, Y. Osamura and H. F. Bettinger, *Astrophys. J.*, 2000, **545**, 892.
- N. Balucani, O. Asvany, Y. Osamura, L. C. L. Huang, Y. T. Lee and R. I. Kaiser, *Planet. Space Sci.*, 2000, **48**, 447.